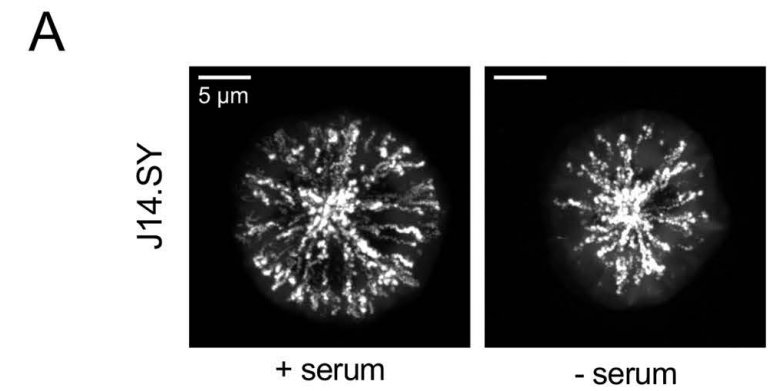

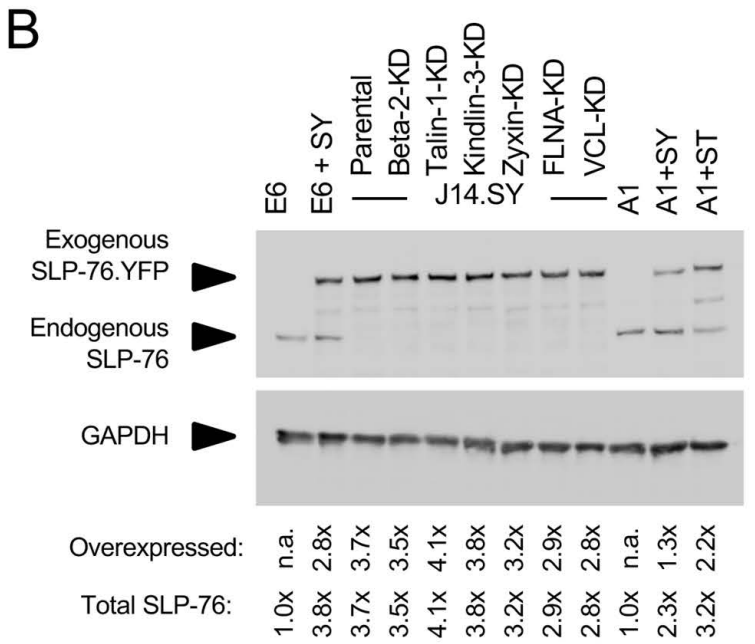

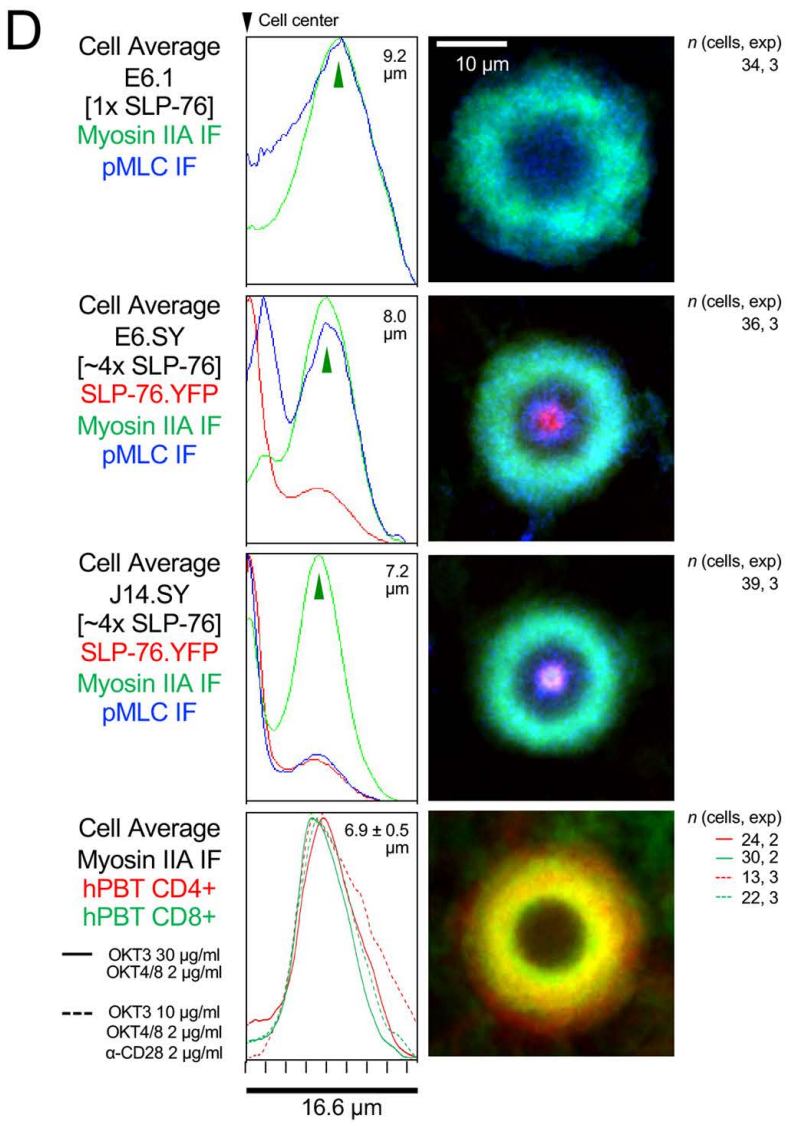

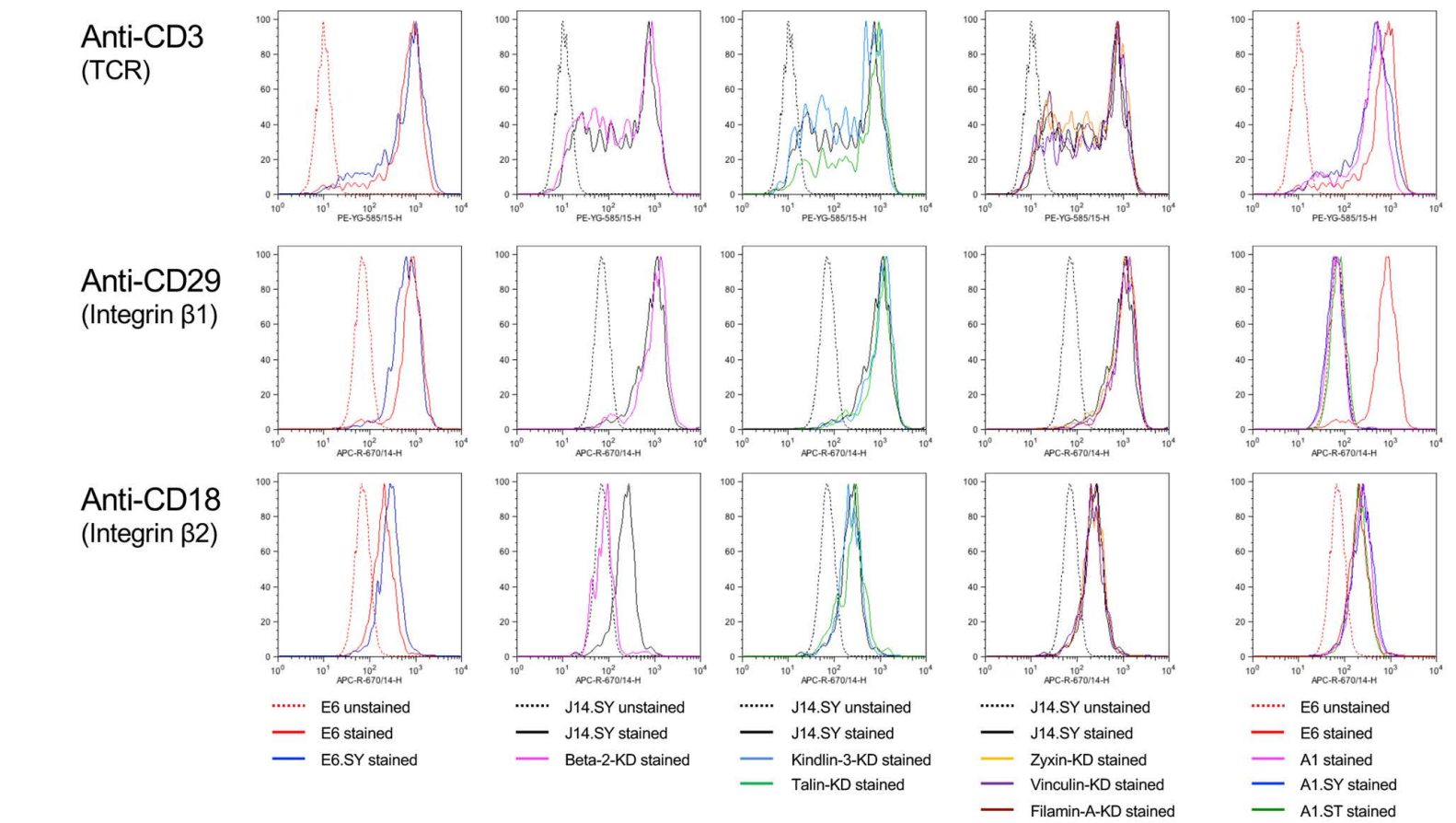

Fig. S1. SLP-76 expression and protein knockdowns regulate the centripetal movement of myosin without affecting key surface markers. (A) J14.SY cells were plated onto 10.0 µg ml-1 OKT3 coated glass wells in the presence or absence of serum and live cell imaged. Representative MOTs are shown. (B-C) Characterization of stable cells lines lacking Kindlin-3, Talin-1, Zyxin, Vinculin, or Filamin-A. (B) E6.1, A1, and J14.SY cells, compared with respective knockdown cell lines were immunoblotted for SLP-76. 'Overexpression' is for the exogenous band, relative to endogenous SLP-76 in the Jurkat E6.1 line; 'Total' includes endogenous SLP-76. (C) Cell lines from B were stained for CD3, CD29, and CD18. (D) Images of cells were center-aligned and averaged to generate composite images. Plots display the average intensities of the indicated proteins as a function of radial distance from the center of the cell. The radial positions of peak myosin IIA fluorescence are indicated. (D, upper panels) Cells acquired for Figure 1B were re-processed as described. (D, bottom panel) Primary human CD4+ and CD8+ T cell blasts were stimulated on substrates coated with antibodies targeting CD3ε, the appropriate co-receptor, and with or without antibodies targeting CD28. Fixed cells were stained for myosin IIA and processed as above. The average radial position (± s.d.) of peak myosin IIA fluorescence across the four conditions is indicated. Three independent experiments were performed in A-C; representative images are shown. The cumulative number of processed cells and the number of experiments from which they originate are displayed in D.

A

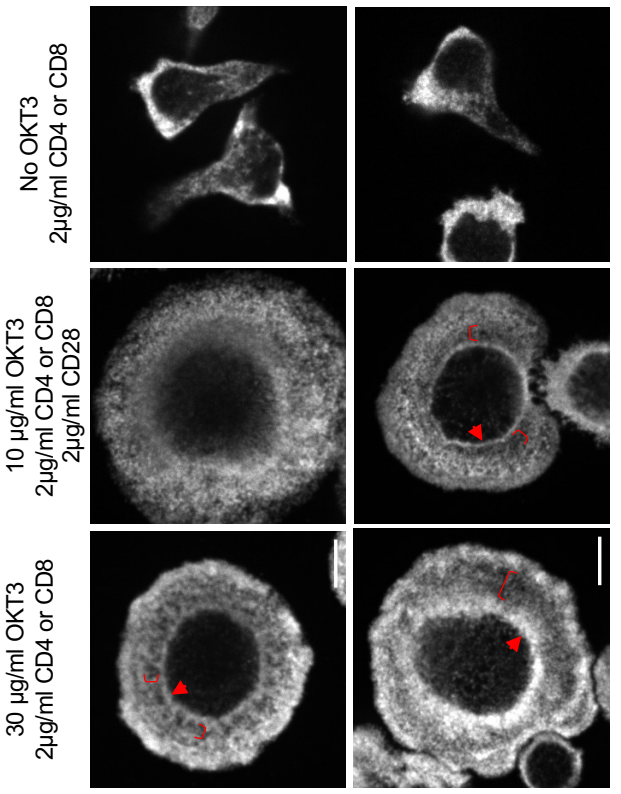

B

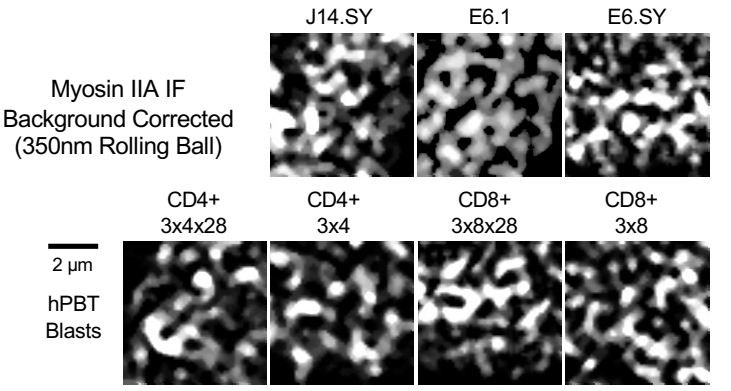

C

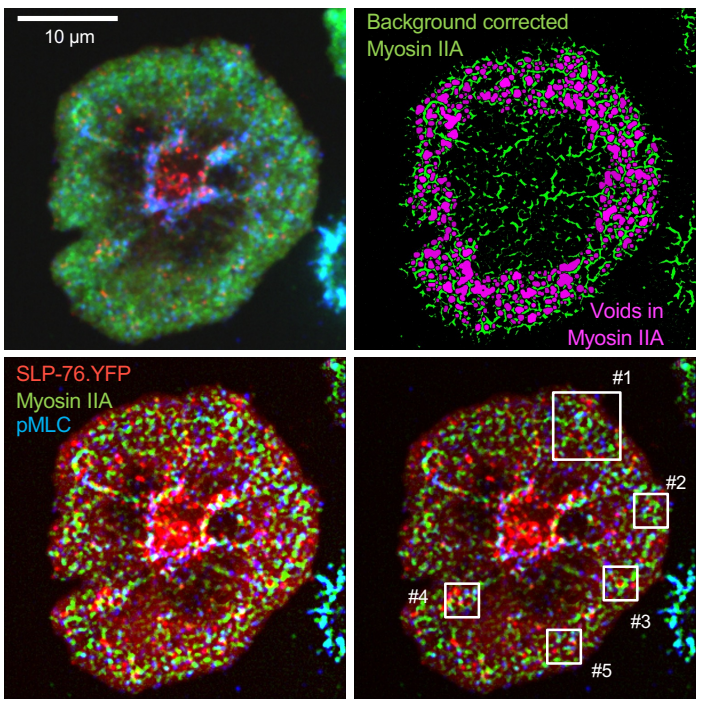

D

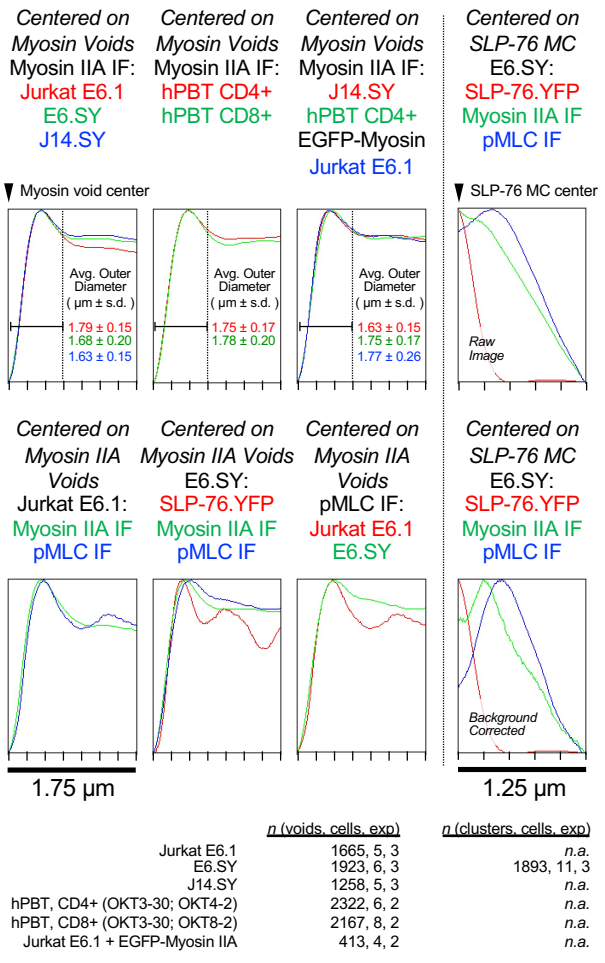

	n (voids, cells, exp)	n (clusters, cells, exp)
Jurkat E6.1	1665, 5, 3	*n.a.*
E6.SY	1923, 6, 3	1893, 11, 3
J14.SY	1258, 5, 3	*n.a.*
hPBT, CD4+ (OKT3-30; OKT4-2)	2322, 6, 2	*n.a.*
hPBT, CD8+ (OKT3-30; OKT8-2)	2167, 8, 2	*n.a.*
Jurkat E6.1 + EGFP-Myosin IIA	413, 4, 2	*n.a.*

E

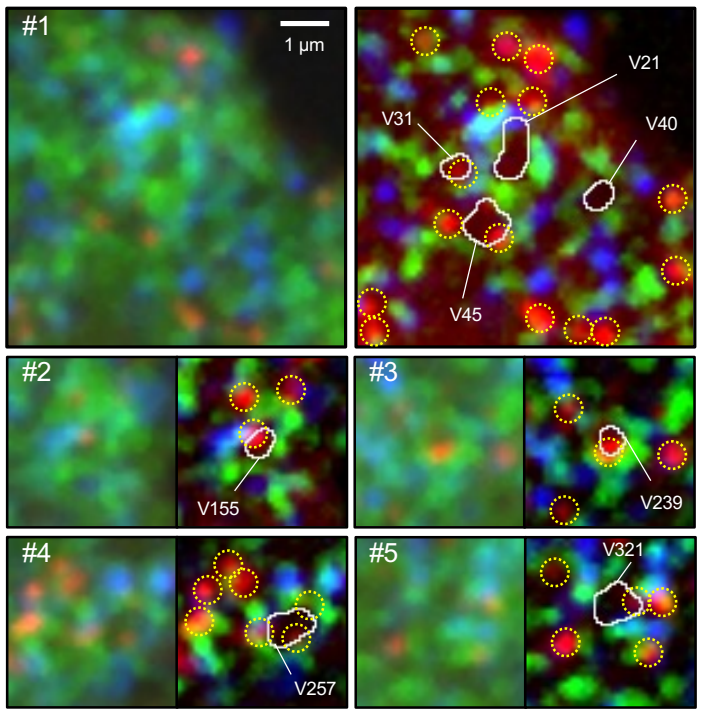

Fig. S2. SLP-76 microclusters are enclosed within or attached to uniformly sized myosin IIA rings. (A) Primary human CD4+ and CD8+ T cells were stimulated and imaged as described in Supplementary Figure 1D (bottom panel). Primary T cells were also stimulated on control substrates coated with co-receptor-specific antibodies (upper two panels). Representative images are shown. Three replicates were performed, except for the high-dose OKT3 condition, where *n*=2. (B) Enlarged, background corrected images were produced as in Figure 1F-G, using images acquired for Figure 1B and Supplementary Figure 2A. (C) Raw images of SLP-76.YFP, myosin IIA, and pMLC in Jurkat E6.1 cells and E6.SY cells were acquired for Figure 1B. Raw images of E6.1 cells expressing EGFP-tagged myosin IIA were acquired for Figure 2C. A representative E6.SY cell is shown (top left). Myosin IIA images were converted into binary masks (green) and 'voids' in the myosin IIA meshwork (magenta) were identified as described in the methods section. The central region of the synapse was excluded because it was not possible to reliably identify filamentous structures in this region (top right). For some subsequent analyses, the myosin IIA and pMLC channels were background corrected using a 350nm rolling ball filter (bottom left). Specific regions analyzed in E, below, are identified with white boxes (bottom right). (D, left) The average intensities of myosin IIA, pMLC, and SLP-76 were captured from raw images as a function of their radial distance from the centers of voids defined using images of myosin IIA. The plots display the average radial intensities of all cells within a group. The outer diameters displayed in the top row are the mean ± s.d. of values determined for myosin IIA in the cells of each group. (D, right) The average intensities of myosin IIA, pMLC, and SLP-76 were captured from raw images (upper) or background corrected images (lower) as a function of their radial distance from the centers of SLP-76 microclusters. The plots display the average radial intensities of all cells within a group. Replicates per condition are listed. (E) Representative raw and background corrected images derived from the cell in panel C, above, are provided to facilitate the interpretation of the data presented in panel D. A subset of the algorithmically identified voids are depicted using white outlines. All of the algorithmically identified SLP-76 microclusters present within these regions are highlighted using dotted yellow circles.

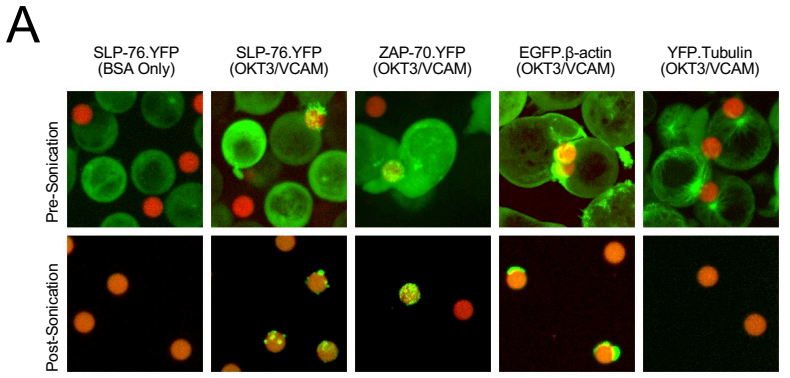

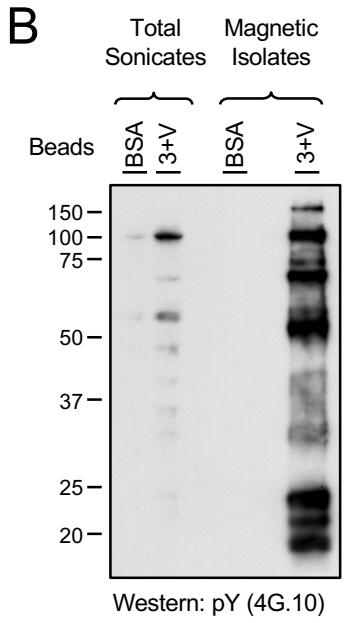

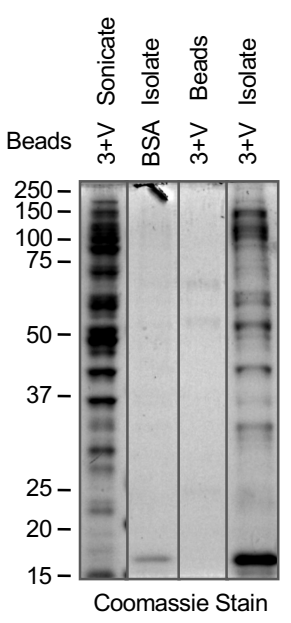

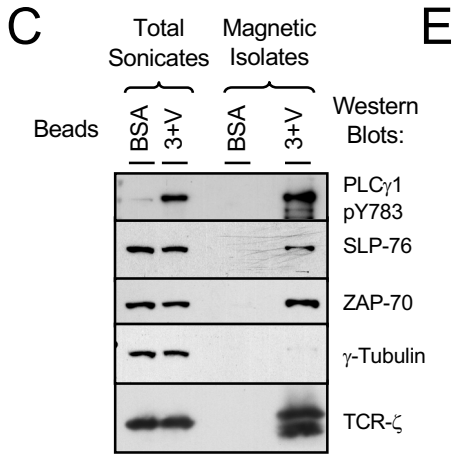

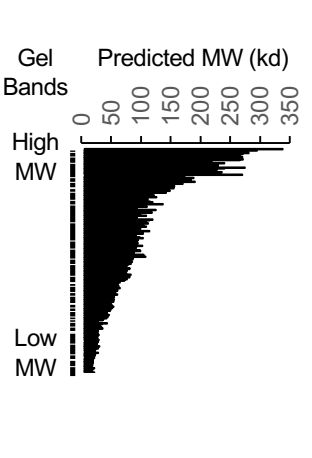

F

Absolute IC	Band #	% Band TIC	Symbol	NCBI ID	Peptides	Description
1.70E+06	30	7.38	ACTB	60	6x	Actin, Beta
1.00E+06	26	6.55	TUBB	203068	1x	Tubulin, Beta
5.00E+05	26	3.21	TUBB4B	10383	5x	Tubulin, Beta 2C
4.70E+05	28	8.34	PA2G4	5036	2x	Erb3BP1
2.60E+05	04	20.83	MYH9	4627	18x	**Myosin IIA**
1.80E+05	03	26.31	TLN1	7094	52x	Talin 1
1.60E+05	26	1.04	TUBA1A	7846	2x	Tubulin, Alpha 10
8.10E+04	02	19.83	FLNB	2317	11x	Filamin-B
5.80E+04	02	14.13	FLNA	2316	11x	Filamin-A
4.80E+04	03	7.15	SPTBN1	6711	10x	Spectrin, Beta
4.40E+04	36	0.18	CLTA	1211	1x	Clathrin Light Chain A
4.30E+04	04	3.36	MYH10	4628	8x	**Myosin IIB**
4.10E+04	12	4.84	LCP2	3937	5x	**SLP-76 (YFP Fusion)**
2.70E+04	26	0.17	CORO1A	11151	1x	Coronin 1A
2.50E+04	06	8.28	CLTC	1213	9x	Clathrin Heavy Chain
2.50E+04	30	0.11	CAPG	822	1x	Capping Protein, Gelsolin-Like
2.40E+04	12	2.77	ACTN4	81	1x	Actinin, Alpha 4
2.40E+04	30	0.11	ACTR2	10097	1x	Arp2 (Arp2/3 Complex)
2.00E+04	02	4.81	SPTAN1	6709	8x	Spectrin, Alpha
1.50E+04	19	0.90	MSN	4478	3x	Moesin
1.30E+04	41	0.59	RAB10	19325	1x	Rab10
9.20E+03	09	2.50	CYFIP2	26999	2x	Pir121/Sra1 (WAVE Complex)
9.20E+03	40	1.30	SEC22B	9554	1x	SEC22B
8.30E+03	40	1.18	RAB5C	5878	2x	Rab5c
7.80E+03	42	2.41	CFL1	476022	2x	Cofilin 1
6.20E+03	40	0.87	RAB11A	8766	3x	Rab11a
4.50E+03	45	0.66	MYL6	281341	2x	**Myosin Light Chain 6**
4.30E+03	05	1.84	IQGAP1	8826	1x	IQGAP
2.40E+03	42	0.74	CD3E	916	1x	**CD3ε (TCR)**
1.80E+03	19	0.11	SEPTIN9	10801	1x	Septin 9
1.50E+03	19	0.09	KIFC1	3833	1x	Kinesin C1
1.20E+03	07	0.10	KTN1	3895	1x	Kinectin 1b
1.10E+03	44	0.16	ARPC5	10092	1x	Arpc5 (Arp2/3 Complex)
8.10E+02	41	0.21	CD3D	915	1x	**CD3δ (TCR)**

G

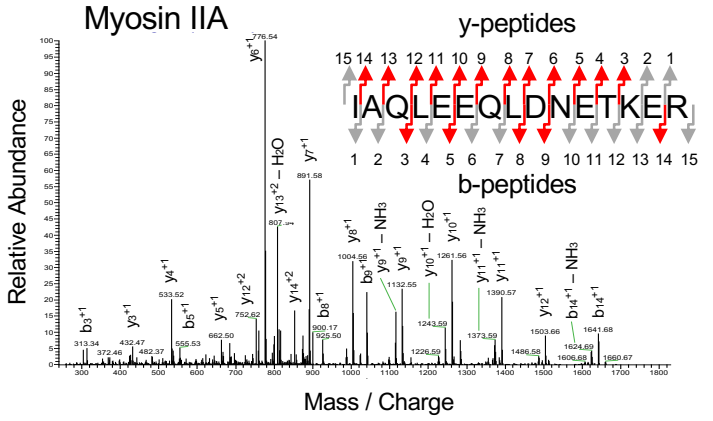

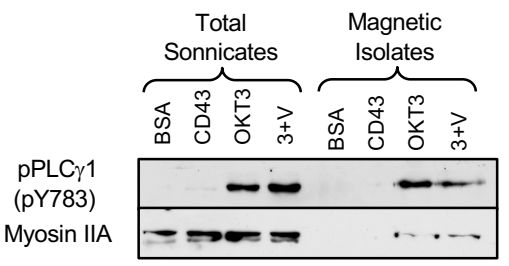

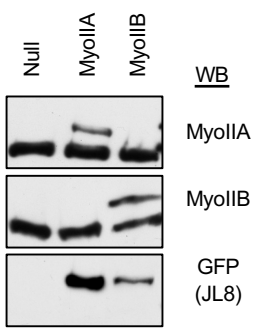

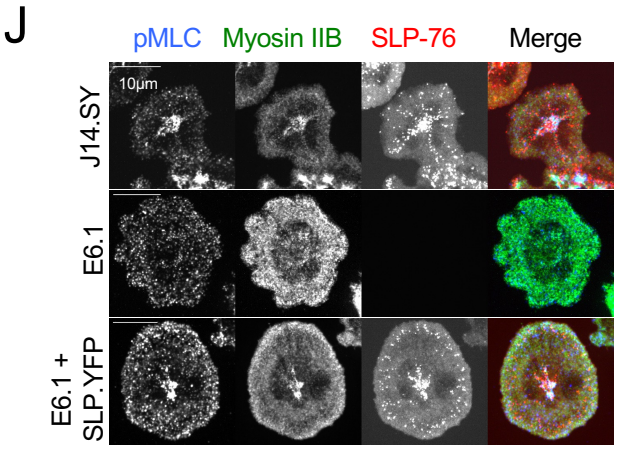

Fig. S3. The magnetic immuno-isolation of integrin-immobilized SLP-76 microclusters and the identification of proteins retained within these structures. (A) Stable T cell lines derived from Jurkat T cell lines were stimulated by co-incubation with 4.5 μm magnetic beads. These lines express stably express SLP-76.YFP (J14.SY), ZAP-70.YFP (E6.ZAP-YFP), EGFP. β-actin (E6.EGFP-Actin), or YFP.Tubulin (E6.YFP-Tubulin). Magnetic beads left untreated or coated with anti-CD3 (OKT3) and recombinant human VCAM-1 and then blocked with BSA. After a 5-minute co-incubation at 37°C, cells were fixed with DSP, a membrane-permeable, lysine-reactive, reversible crosslinking agent. After fixation, cells were disrupted by sonication, and bead-attached signaling complexes were purified from the total lysate by magnetic isolation. The bead-cell conjugates and bead-attached signaling complexes obtained pre- and post-sonication were visualized by confocal microscopy. Representative top-down projections of image stacks spanning 30 μm are shown. Fluorescent proteins are pseudocolored green; magnetic beads are pseudocolored red. (B-C) Total sonicates ($2x10^5$ cell equivalents) and magnetic isolates ($2x10^7$ cell equivalents) derived from J14.SY cells were examined by western blotting. (D) The same total sonicates, beads, and bead isolates were analyzed by Coomassie staining. (E-G) Slices cut from the rightmost lane of the gel in D were reduced, alkylated, and trypsinized in-gel. LC/MS/MS analysis was performed using a Thermo LTQ ion trap mass spectrometer. MS/MS spectra were searched against the NCBI non-redundant protein sequence database using the SEQUEST computer algorithm. (E) The predicted molecular weights of identified proteins accurately track their initial positions in the gel. (F) Table depicting the most abundant hits with roles in signal transduction, cytoskeletal function, and membrane transport. A complete list of hits is provided in Supplementary Table S2. Bands were numbered from top to bottom; thus, high molecular weight proteins have low band numbers. Absolute IC is cumulative ion current associated with all peptides contributing to a given hit. Percent band TIC is fraction of the total ion current associated with a given band that is contributed by a given hit. Peptides is the number of unique peptides that could be non-redundantly assigned to each hit. (G) A representative fragmentation spectrum for one of the peptides contributing to the identification of Myosin IIA in our magnetic immuno-isolates. (H) Total sonicates and magnetic isolates were independently derived from J14.SY cells and examined by western blotting. Samples were prepared using control BSA-coated beads (BSA) and beads coated with anti-CD3, either with (3+V) or without VCAM-1 (OKT3). A specificity control was provided by using beads coated with a non-stimulatory but pro-adhesive ligand, anti-CD43 (CD43). (I) Jurkat E6.1 cells were transiently transfected with EGFP-tagged myosin IIA (MyoIIA) or IIB (MyoIIB) and lysates blotted as indicated. (J) J14.SY cells, E6.1 cells, E6.1 cells stably transduced with SLP-76.YFP were stimulated as Fig. 1B, fixed after 7 minutes, and stained for myosin IIB and pMLC.

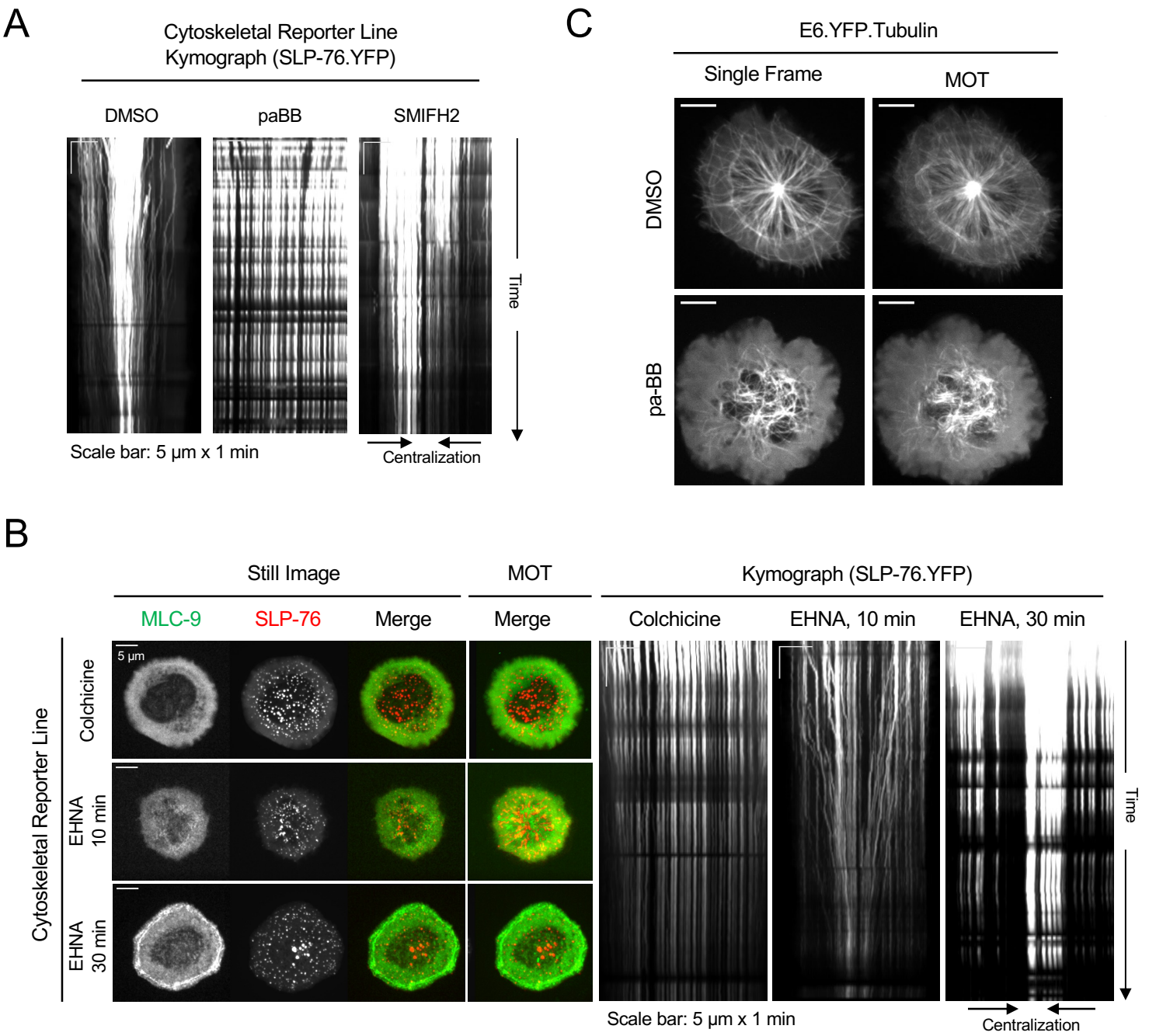

Fig. S4. Myosin ATPase activity, formin function, intact microtubules and dynein ATPase activity are required for the co-accumulation of SLP-76 microclusters and contractile myosin filaments at the center of the contact. (A) J14.SY-CRL cells were pretreated for 30 minutes with DMSO, or para-amino-blebbistatin (paBB, 50 µM), or for 10 minutes with SMIFH2 (25 µM) and then stimulated on substrates coated with anti-CD3 (10.0 µg ml^{-1}) and anti-CD43 (10.0 µg ml^{-1}). Each channel was imaged every 5.6 seconds for 150 frames (14 min). Kymographs track SLP-76 microcluster movement in the image stacks corresponding to Fig. 2I. (B) J14.SY-CRL cells were pretreated for 60 minutes with DMSO, or Colchicine (100 µM), or for 10 or 30 minutes with EHNA (1mM) and then stimulated on substrates coated with anti-CD3 (10.0 µg ml^{-1}) and anti-CD43 (10.0 µg ml^{-1}). Each channel was imaged every 5.6 seconds for 150 frames (14 min). (C) E6.YFP.Tubulin cells were pretreated with DMSO or with para-amino-blebbistatin (paBB, 50 µM) for 30 minutes and then plated onto OKT3 coated glass wells (10.0 µg ml^{-1}) and live cell imaged. YFP channel was collected every 2 seconds for 150 frames. Two replicates performed. Identical results were observed in three additional replicates using blebbistatin (50 µM)

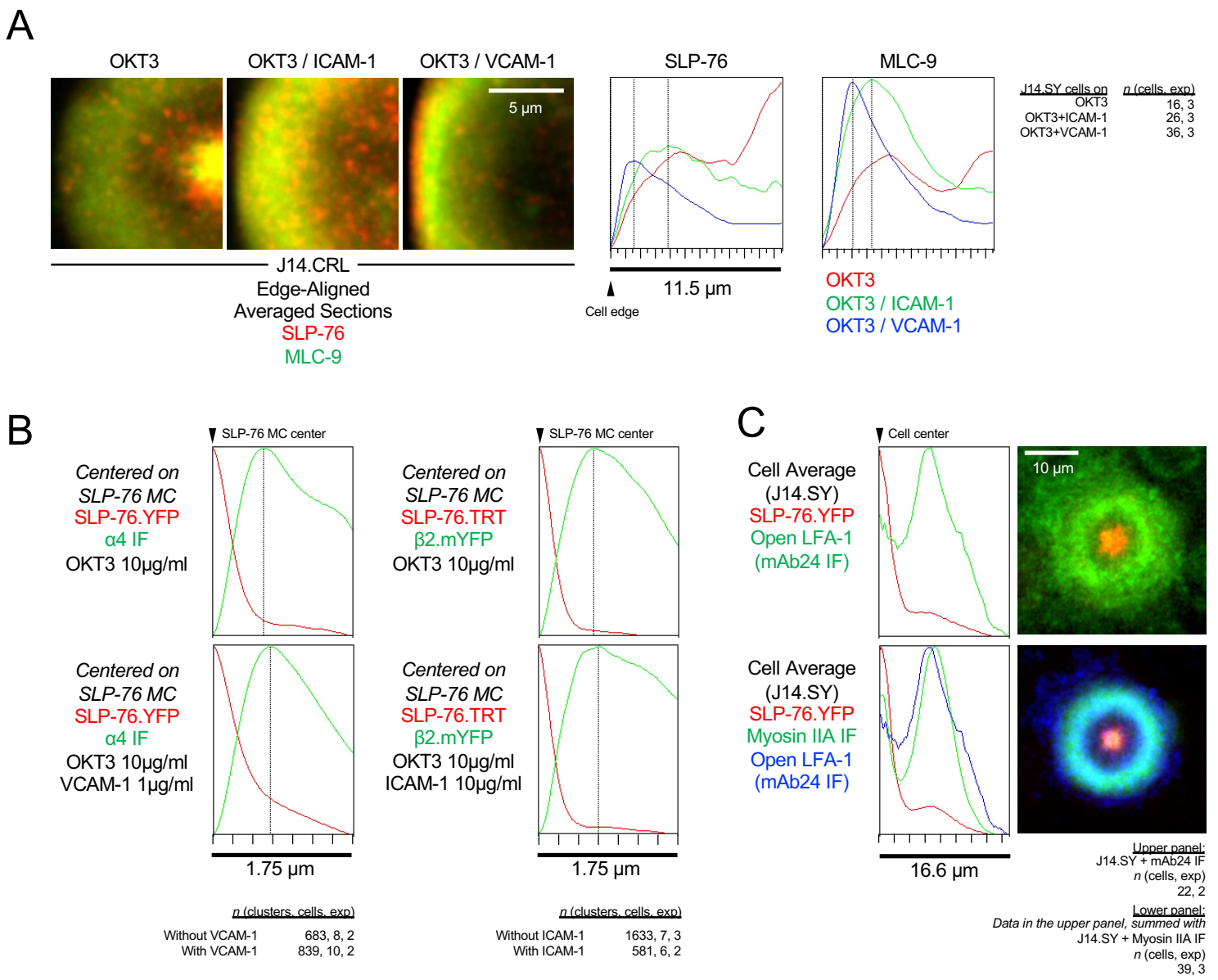

Fig. S5. Integrins impact the movement of SLP-76 microclusters despite being excluded from SLP-76 microclusters. (A) Regions acquired from the images obtained for Fig. 3B were aligned via the outer boundaries of cells and averaged (left panels). These images were then integrated vertically to generate fluorescence intensity profiles as a function of distance from the cell edge (right panels). (B) Radial intensity profiles relative to the centers of SLP-76 microclusters were generated from raw images. (B, left) A subset of the J14.SY cells analyzed in Fig. 3D were processed to generate radial intensity profiles. Cells were stimulated as indicated, fixed, and stained with α4. (B, right) J14.ST cells transiently transfected with β2.mYFP and α4.mCFP were stimulated as indicated, imaged with or without fixation, and processed to generate radial intensity profiles. (C) J14.SY cells stimulated on substrates coated with 10 µg ml^{-1} OKT3 were stained with mAb24, fixed, and imaged. Because the staining with mAb24 was weak, images were center-aligned and averaged to generate composite images. The upper plot displays the average intensities of SLP-76.YFP and mAb24 as functions of radial distance from the center of the cell. For comparison, the lower panel sums this data with the J14.SY cells analyzed for myosin IIA in Fig. S1D. Replicate information is provided in all panels.

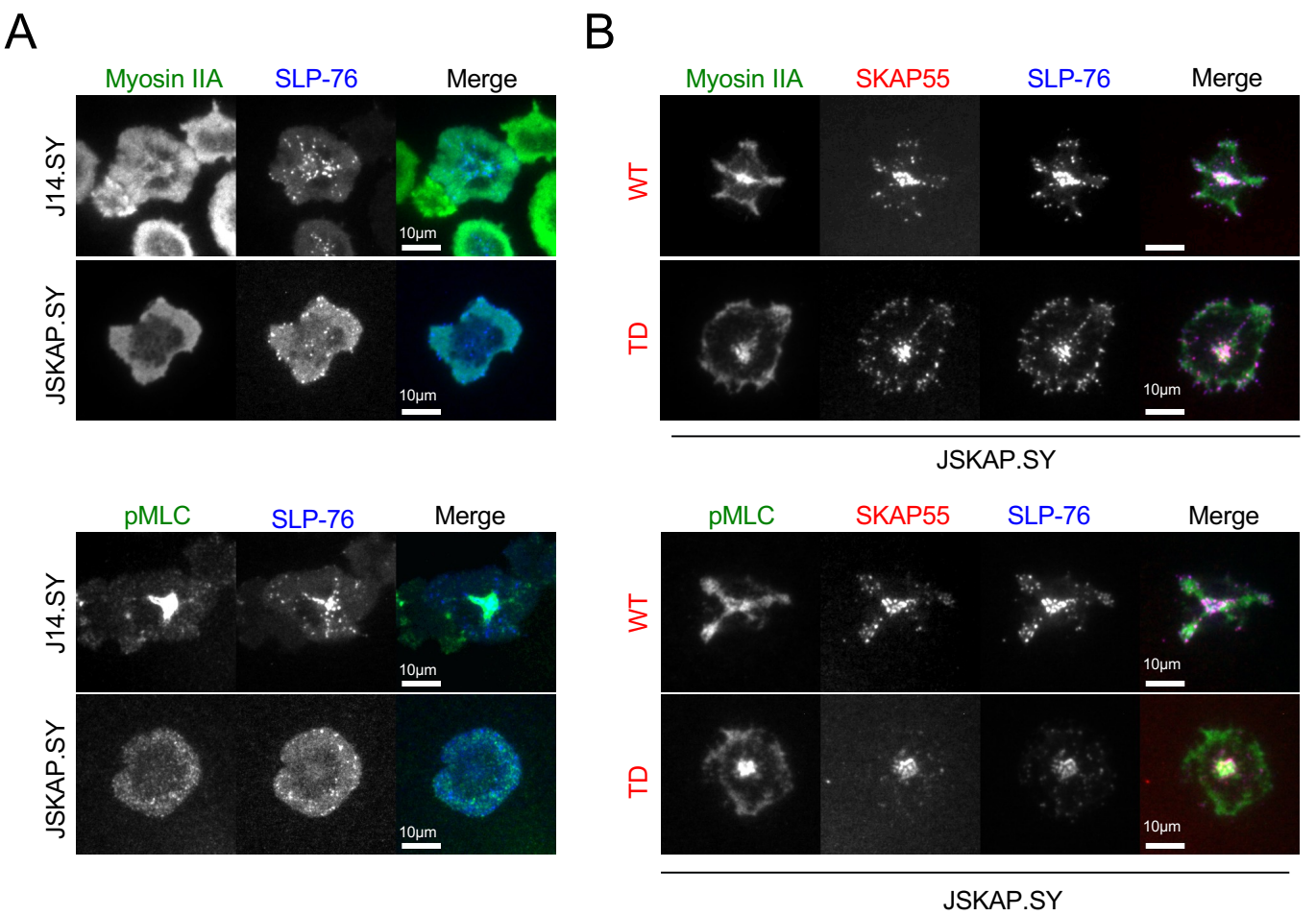

Fig. S6. The N-terminus of SKAP55 is dispensable for SLP-76 microcluster centralization and the central accumulation of contractile myosin. (A) The parental J14.SY cell line and its SKAP55-deficient derivative JSKAP.SY were stimulated on anti-CD3 coated glass substrates, fixed, and stained for either myosin IIA or phospho-MLC (pMLC). Representative images are shown, n=3. (B) JSKAP.SY cells were transiently transfected with either wild-type full length SKAP55 or with the tandem-dimer (TD) construct and stimulated, fixed, and stained as in A. Representative images are shown, Two replicates performed.

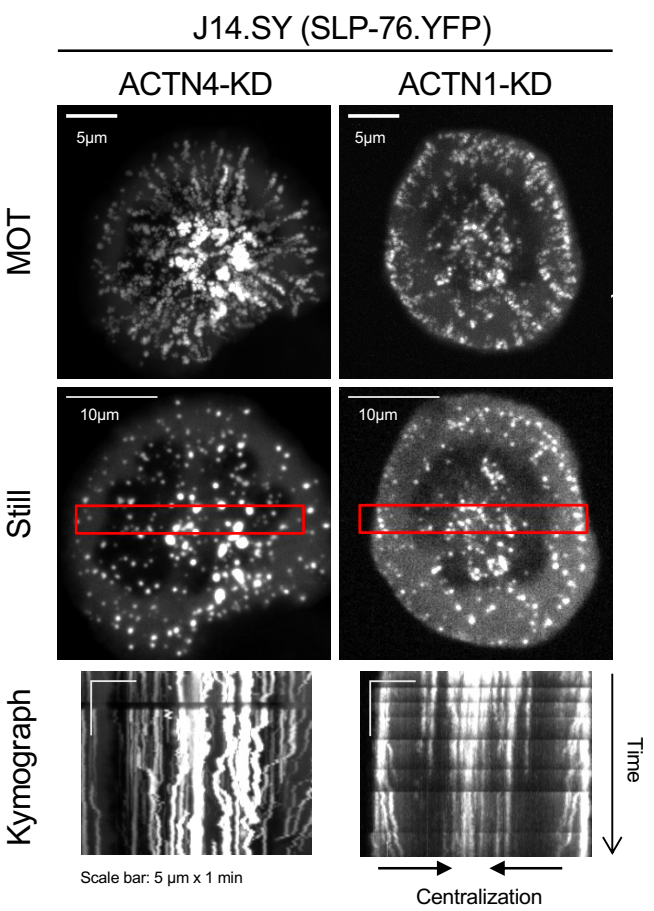

Fig. S7. α- Actinin-1 and α- Actinin-4 play roles in SLP-76 microcluster centralization. JJ14.SY cells were stably transduced with shRNAs targeting α-Actinin-4 (ACTN4) or α-Actinin-1 (ACTN1). These cells were stimulated on anti-CD3 coated glass substrates. SLP-76.YFP was imaged every 2 seconds for 150 frames (5 min). Representative still images and maximum-over-time (MOT) projections are shown; kymographs were derived from the indicated regions, n=2.

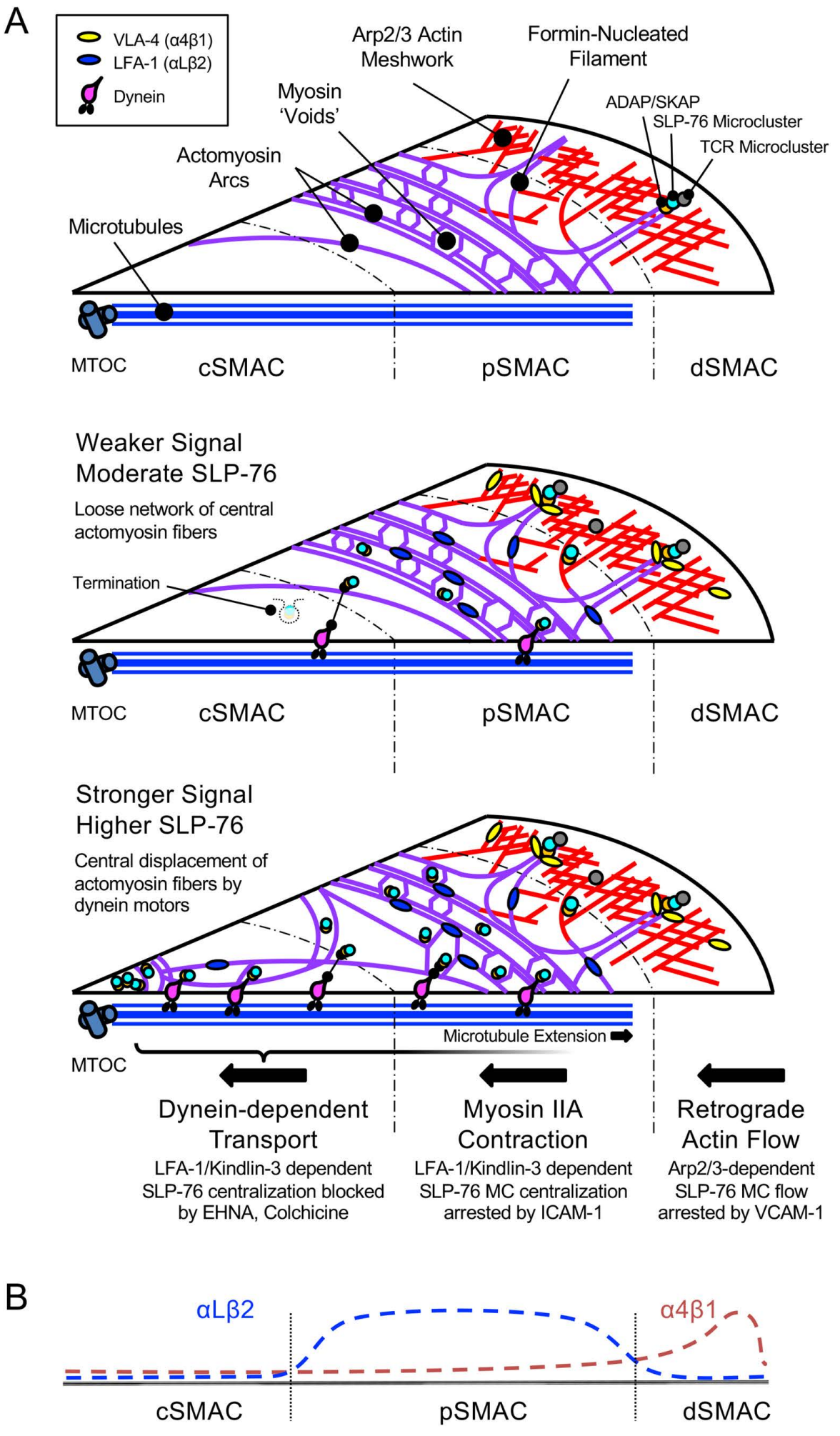

Fig. S8. A model linking SLP-76 microclusters movement to cytoskeletal systems via LFA-1. (A) Distal TCR engagement gives rise to TCR (grey circles) and SLP-76 (cyan circles) microclusters; SLP-76 microclusters recruit ADAP and SKAP55 (orange circles) which interact with F-actin and activate integrins. In the absence of integrin ligands, SLP-76 microclusters separate from TCR microclusters and are transported to the center of the synapse. In the absence of VCAM-1, SLP-76 microclusters are swept through the dSMAC by Arp2/3-dependent actin treadmilling. Subsequently, in the absence of ICAM-1, SLP-76 microclusters move through the pSMAC. During this process, SLP-76 microclusters interact with the margins of small (~1.75 μm) actomyosin rings, which are integrated into circumferential actomyosin arcs. LFA-1 (blue ovals) is directly incorporated into these arcs. Once SLP-76 microclusters exit the pSMAC, they can be internalized and terminated (upper panel) or can accumulate in the center of the contact (lower panel). In synapses induced by weak TCR ligands, the cSMAC is sparsely populated by actin filaments and SLP-76 microclusters do not reach the center of the contact. In contrast, when the TCR is potently stimulated and when SLP-76 is abundant, SLP-76 microclusters and contractile myosin filaments translocate towards the cSMAC. The latter process requires formins, myosin II, dynein, kindlin-3, and the kindlin-3-binding site in LFA-1, but does not require talin. We propose that persistent SLP-76 microclusters interact with dynein via ADAP, and thereby transmit dynein-dependent forces to formin-dependent actomyosin arcs within the pSMAC. If these forces exceed the tensile strength of these arcs, the arcs deform and rupture, allowing actomyosin filaments to accumulate in the center of the synapse. Conversely, the myosin-dependent rigidification of the lamellar actomyosin network may enable microcluster-associated dynein motors to polarize the MTOC and to drive microtubules into the periphery of the synapse. (B) A model describing the presumed locations of active integrins within the immune synapse.

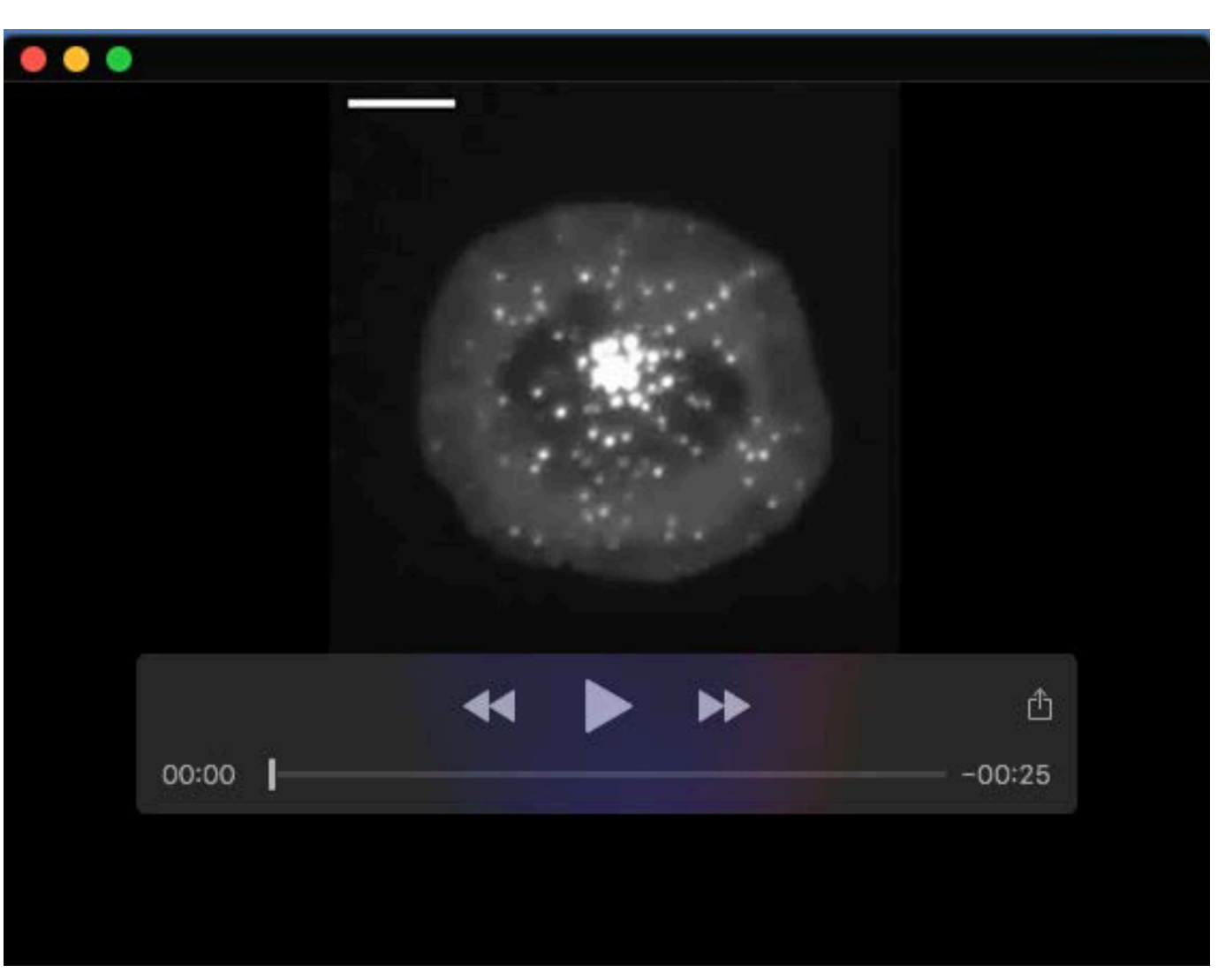

Movie 1. Live cell imaging of J14.SY cells plated on anti-CD3 coated glass wells. Wild-type J14.SY cells were stimulated on anti-CD3 coated glass substrates. SLP-76.YFP was imaged every 2 seconds for 150 frames (5 min). Movies play at 0.06 s frame^{-1}, yielding a 33.3x compression rate. Scale bar is 5 μm.

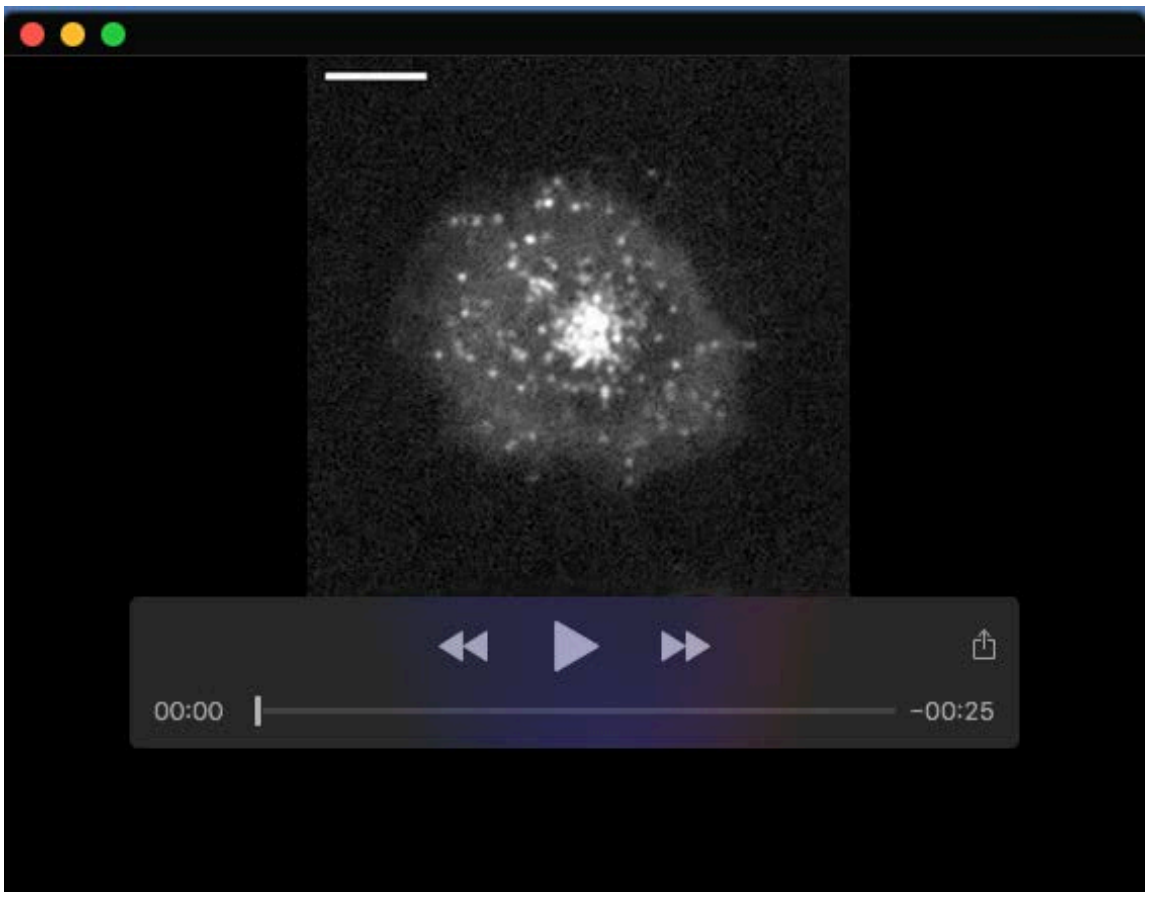

Movie 2. Live cell imaging of A1.ST cells plated on anti-CD3 coated glass wells. β1-deficient A1.ST cells were stimulated on anti-CD3 coated glass substrates. SLP-76.TRT was imaged every 2 seconds for 150 frames (5 min). Movies play at 0.06 s frame^{-1}, yielding a 33.3x compression rate. Scale bar is 5 µm.

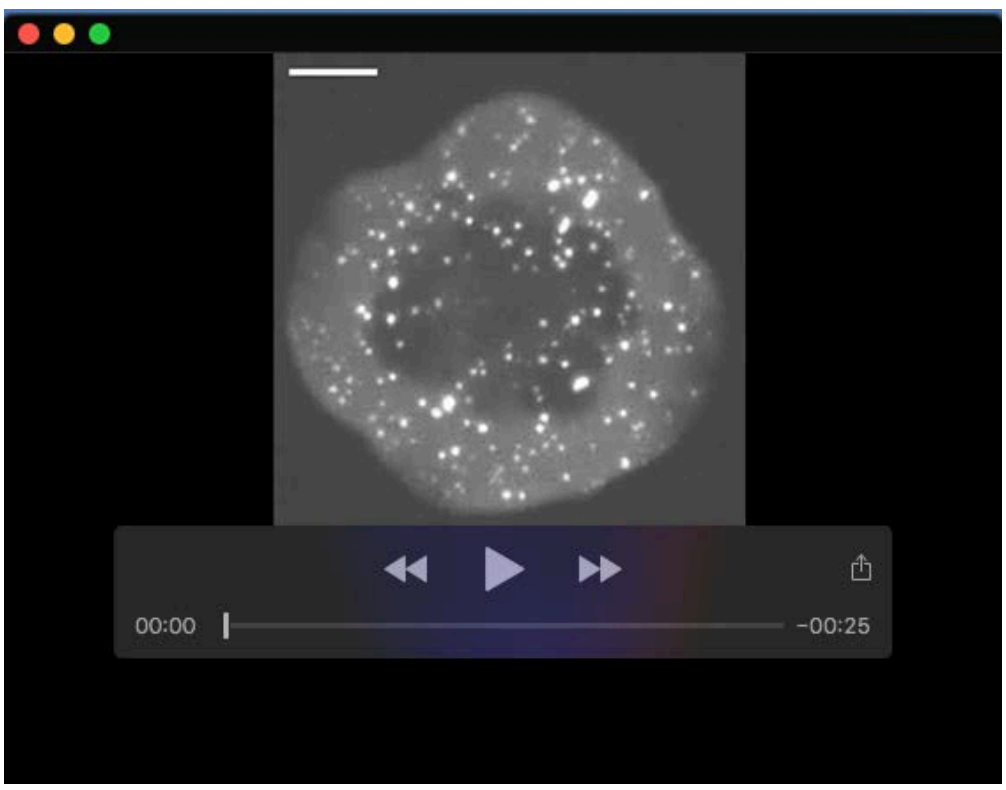

Movie 3. Live cell imaging of β2 knockdown cells plated on anti-CD3 coated glass wells. J14.SY cells were stably transduced with a shRNA targeting β2. Cells were stimulated on anti-CD3 coated glass substrates. SLP-76.YFP was imaged every 2 seconds for 150 frames (5 min). Movies play at 0.06 s frame^{-1}, yielding a 33.3x compression rate. Scale bar is 5 µm.

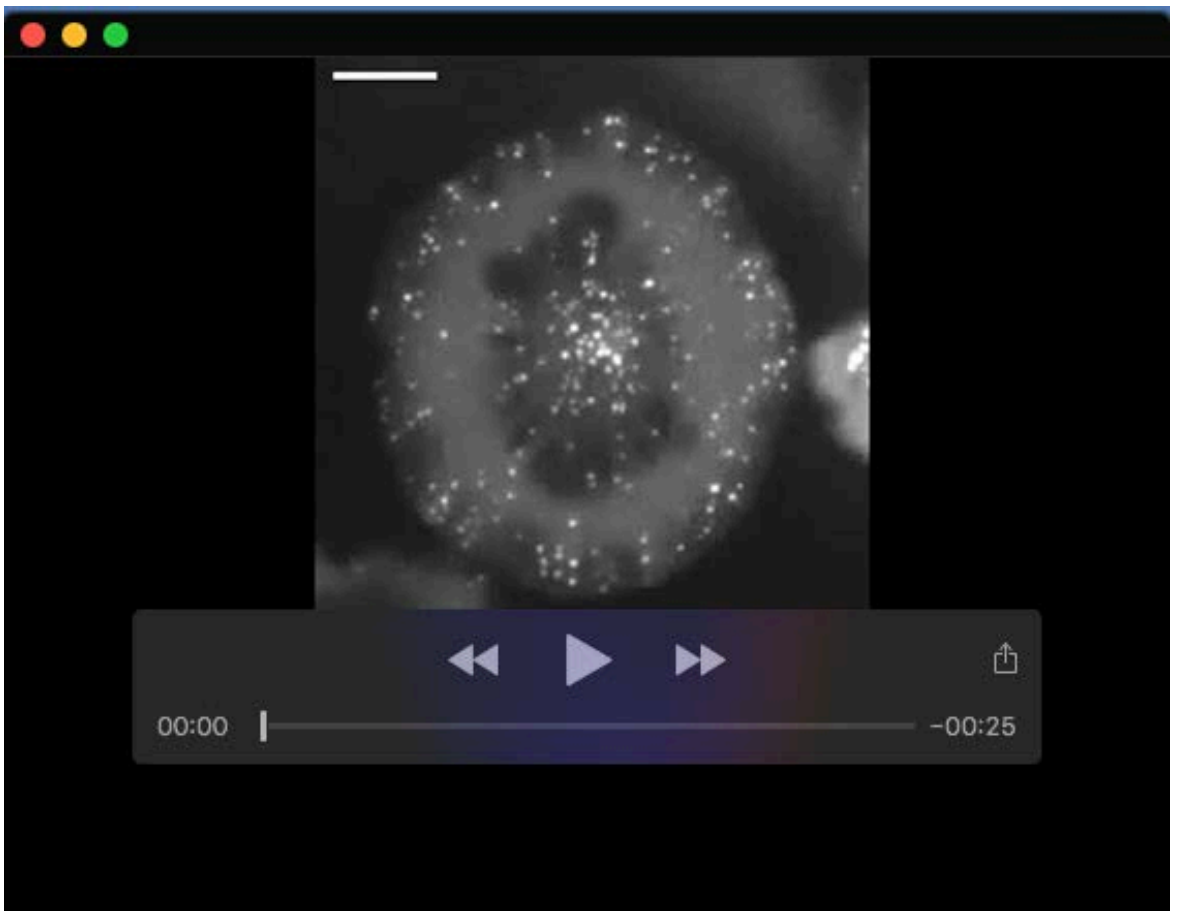

Movie 4. Live cell imaging of Talin-1 knockdown cells plated on anti-CD3 coated glass wells. J14.SY cells were stably transduced with a shRNA targeting Talin-1. Cells were stimulated on anti-CD3 coated glass substrates. SLP-76.YFP was imaged every 2 seconds for 150 frames (5 min). Movies play at 0.06 s frame^{-1}, yielding a 33.3x compression rate. Scale bar is 5 µm.

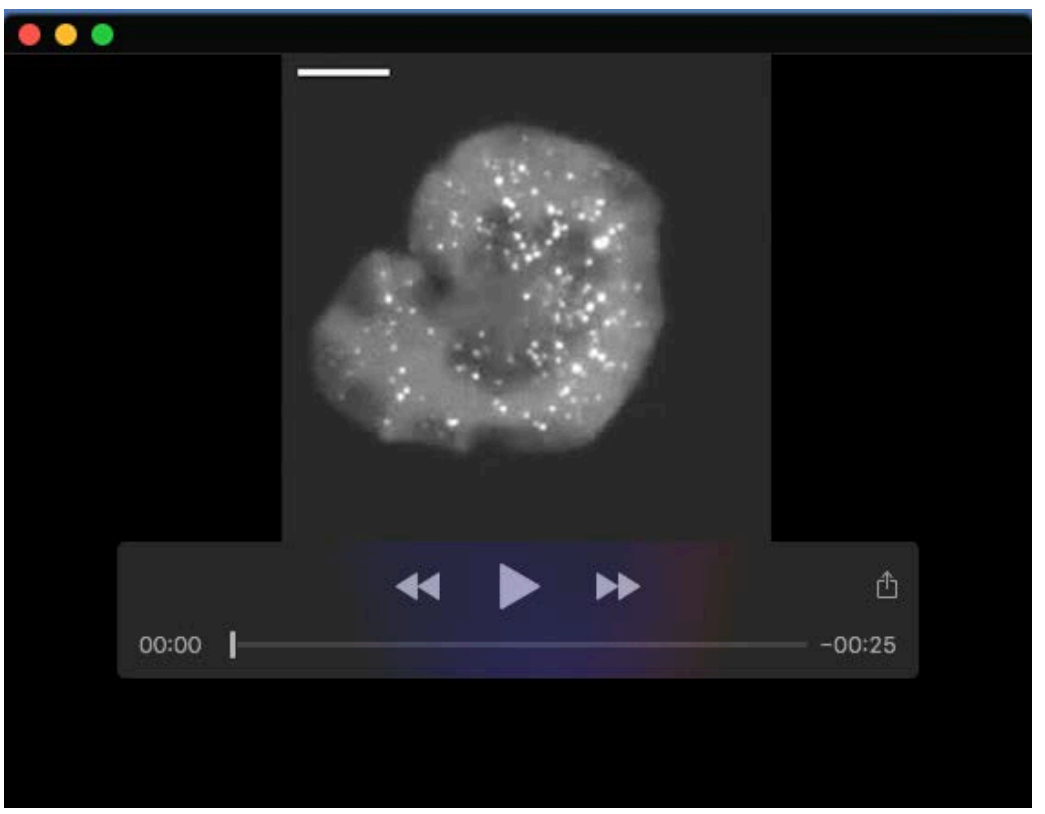

Movie 5. Live cell imaging of Kindlin-3 knockdown cells plated on anti-CD3 coated glass wells. J14.SY cells were stably transduced with a shRNA targeting Kindlin-3. Cells were stimulated on anti-CD3 coated glass substrates. SLP-76.YFP was imaged every 2 seconds for 150 frames (5 min). Movies play at 0.06 s frame^{-1}, yielding a 33.3x compression rate. Scale bar is 5 µm.

Journal of Cell Science • Supplementary information

Table S1. Oligonucleotides used in vector construction

Oligo ID	Oligo Name	Sequence
Oligos for MYH9 shRNA assembly		
NRS801	MYH9.shRNA-1.f1	GATCCGGCCAAACCTGCCGAATAAt t caagaga
NRS802	MYH9.shRNA-1.r1	ATAAt ct ct t gaaTTATTCGGCAGGTTTGGCCG
NRS803	MYH9.shRNA-1.f2	TTATTCGGCAGGTTTGGCCTTTTTGGA
NRS804	MYH9.shRNA-1.r2	AGCTTCCAAAAAGGCCAAACCTGCCGA
Oligos for H1p-shRNA cassette amplification		
NRS753	H1-shRNA.Rescue-5'-NdeI.f	gacagcCATATGCGAACGCTGACGTCATCAACC
NRS754	H1-shRNA.Rescue-3'-AseI.r	ggcaaggcATTAATCGACGGt at cgAt AAGCTTCC
Oligos for the production of tailless b2.mYFP		
KPE017	Beta2.f1	GACTGAATTCGACTACCCATCGGTGGGC
KPE018	Beta2.r1	CACATAGATGAGGTAcCGGTCCATCCCGT
Gibson primers for Beta-2 tail mutants		
KPEG026	b2-NPLF/AAAA	ACGCTGGAGCAGCAGGACGGGATGGACCGGt ACCTCATCTA TGTGGATGAGAGCCGAGAGTGTGTGGCAGGCCCCAACATCG CCGCCATCGTCGGGGGCACCGTGGCAGGCATCGTGCTGATC GGCATTCTCCTGCTGGTCATCTGGAAGGCTCTGATCCACCT GAGCGACCTCCGGGAGTACAGGCGCTTTGAGAAGGAGAAGC TCAAGTCCCAGTGGAACAATGATaat ccccttttcAAGAGC GCCACCACGACGGTCATGgct gct gccgcaGCTGAGAGTgg cggaCCGGTCGCCACCATGGTGAGCAAGGGCGAG
KPEG027	b2-AAAA/NPKF	ACGCTGGAGCAGCAGGACGGGATGGACCGGt ACCTCATCTA TGTGGATGAGAGCCGAGAGTGTGTGGCAGGCCCCAACATCG CCGCCATCGTCGGGGGCACCGTGGCAGGCATCGTGCTGATC GGCATTCTCCTGCTGGTCATCTGGAAGGCTCTGATCCACCT GAGCGACCTCCGGGAGTACAGGCGCTTTGAGAAGGAGAAGC TCAAGTCCCAGTGGAACAATGATgcagcagct gccAAGAGC GCCACCACGACGGTCATGaaccccaagtttGCTGAGAGTgg cggaCCGGTCGCCACCATGGTGAGCAAGGGCGAG
KPEG028	b2-AAAA/AAAA	ACGCTGGAGCAGCAGGACGGGATGGACCGGt ACCTCATCTA TGTGGATGAGAGCCGAGAGTGTGTGGCAGGCCCCAACATCG CCGCCATCGTCGGGGGCACCGTGGCAGGCATCGTGCTGATC GGCATTCTCCTGCTGGTCATCTGGAAGGCTCTGATCCACCT GAGCGACCTCCGGGAGTACAGGCGCTTTGAGAAGGAGAAGC TCAAGTCCCAGTGGAACAATGATgcagcagct gccAAGAGC GCCACCACGACGGTCATGgct gct gccgcaGCTGAGAGTgg cggaCCGGTCGCCACCATGGTGAGCAAGGGCGAG

Table S2. Proteomic characterization of signaling complexes induced via the co-ligation of the TCR and VLA-4. The unique proteins and peptides identified in Fig. S3 are listed by source band. The molecular weights of the parent proteins are shown. Some peptides are present in more than one band. For each protein, the total number of unique peptides across all bands and the number of unique peptides in the relevant band are shown. The %TIC in Band is the fraction of the band-specific ion current that is derived from all of the peptides associated with a specific protein.

Click here to download Table S2